NMR Studies of the AMP-Binding Site and Mechanism of Adenylate Kinase†

David C. Fry,‡ Stephen A. Kuby,§ and Albert S. Mildvan*,‡

Department of Biological Chemistry, Johns Hopkins University School of Medicine, Baltimore, Maryland 21205, and Laboratory for the Study of Hereditary and Metabolic Disorders and Departments of Biological Chemistry and Medicine, University of Utah, Salt Lake City, Utah 84108

Received July 14, 1986; Revised Manuscript Received October 23, 1986

ABSTRACT: NMR has previously been used to determine the conformation of enzyme-bound MgATP and to locate the MgATP-binding site on adenylate kinase [Fry, D. C., Kuby, S. A., & Mildvan, A. S. (1985) *Biochemistry 24*, 4680–4694]. To determine the conformation and location of the other substrate, AMP, distances have been measured from Cr^{3+}AMPPCP, a linear competitive inhibitor with respect to MgATP, to six protons and to the phosphorus atom of AMP on adenylate kinase, with the paramagnetic probe–T_1 method. Time-dependent nuclear Overhauser effects (NOEs) have been used to measure five interproton distances on enzyme-bound AMP. These distances were used to determine the conformation of bound AMP in addition to its position with respect to metal–ATP. Enzyme-bound AMP exhibits a high *anti*-glycosyl torsional angle ($\chi = 110 \pm 10°$), a 3′-endo,2′-exo ribose pucker ($\delta = 105 \pm 10°$), and gauche–trans orientations about the C4′–C5′ bond ($\gamma = 180 \pm 10°$) and the C5′–O5′ bond ($\beta = 170 \pm 20°$). The distance from Cr^{3+} to the phosphorus of AMP is 5.9 ± 0.3 Å, indicating a reaction coordinate distance of ~3 Å, which is consistent with an associative S_N2 mechanism for the phosphoryl transfer. Ten intermolecular NOEs, from protons of the enzyme to those of AMP, were detected, indicating the proximity of at least three hydrophobic amino acids to bound AMP. These constraints, together with the conformation of AMP and the intersubstrate distances, were used to position AMP into the X-ray structure of adenylate kinase. The AMP binding site is found to be near (≤4 Å from) Leu-116, Arg-171, Val-173, Val-182, and Leu-190; all of these residues have been found to be invariant in muscle-type rabbit, calf, human, porcine [Kuby, S. A., Palmieri, R. H., Frischat, A., Fischer, A. H., Wu, L. H., Maland, L., & Manship, M. (1984) *Biochemistry 23*, 2393–2399], and chicken adenylate kinase [Kishi, F., Maruyama, M., Tanizawa, Y., & Nakazawa, A. (1986) *J. Biol. Chem. 261*, 2942–2945].

Adenylate kinase catalyzes the transfer of a phosphoryl group in the reversible reaction

$$MgATP + AMP \rightleftharpoons MgADP + ADP$$

The enzyme contains two distinct substrate binding sites, one of which binds MgATP and MgADP and the other of which is specific for uncomplexed AMP and ADP (Hamada & Kuby, 1978; Rhoads & Lowenstein, 1968; Nageswara Rao et al., 1978). The location of these binding sites on the enzyme has been a problem of ongoing interest to this laboratory. We have recently determined the binding site of MgATP on rabbit muscle adenylate kinase (Fry et al., 1985) through an extensive NMR study in solution of both the intact enzyme and a synthetic peptide, comprising amino acid residues 1–45 of the enzyme. This peptide binds Cr^{3+}ATP and magnesium 1,N^6-ethenoadenosine 5′-triphosphate (MgϵATP)[1] with affinities comparable to those of the entire enzyme (Fry et al., 1985; Hamada et al., 1979). The metal–ATP binding site determined by NMR was substantially different from that based on X-ray studies of the binding site of salicylate (Pai et al., 1977). In fact, it more closely resembled the site that had been designated by the crystallographers as the AMP-binding site. This latter designation was based upon the binding of MnATP that had been diffused into crystals of adenylate kinase and the assumption that the MnATP had hydrolyzed to AMP during this process (Pai et al., 1977).

In light of the extensive overlap between the AMP-binding site as proposed from the X-ray studies and the corrected metal–ATP binding site determined by NMR, a reevaluation of the location of the AMP-binding site was necessary. Therefore, we have studied AMP bound to adenylate kinase in two ways. First, we have determined its orientation with respect to bound Cr^{3+}AMPPCP, by using the paramagnetic probe–T_1 method to measure distances from Cr^{3+} to the phosphorus and protons of AMP. These intersubstrate distances also permitted an estimate of the lower limit reaction coordinate distance, from the entering phosphate oxygen of AMP to the γ-phosphorus of metal–ATP, providing valuable mechanistic information. Second, we have used nuclear Overhauser experiments to refine the conformation of bound AMP and to obtain a set of proximities between the protons of AMP and those of enzyme side chains. Using the X-ray structure of the enzyme (Sachsenheimer & Schulz, 1977) and our previously determined binding site for Cr^{3+}ATP (Fry et al., 1985), we have located a unique site within the enzyme at which the proper conformation of AMP can bind and satisfy all of the distance constraints provided by the NMR data. A

† This work was supported by National Institutes of Health Grants AM28616 and AM07824. We also acknowledge the use of the Interactive Graphics Facility of the Department of Biophysics that was established and maintained by NIH and NSF grants and by a gift from the Richard-King Mellon Foundation.

* Author to whom correspondence should be addressed.

‡ Johns Hopkins University School of Medicine.

§ University of Utah.

[1] Abbreviations: CrAMPPCP, β,γ-bidentate chromium(3+) adenosine 5′-(β,γ-methylenetriphosphate); ϵATP, 1,N^6-ethenoadenosine 5′-triphosphate; DTT, dithiothreitol; DSS, sodium 4,4′-dimethyl-4-silapentanesulfonate; pH*, pH meter reading in ^2H_2O; A/D, analog to digital; NOE, nuclear Overhauser effect; Tris, tris(hydroxymethyl)aminomethane; DTE, dithioerythritol; EDTA, ethylenediaminetetraacetic acid.

0006-2960/87/0426-1645$01.50/0

preliminary account of this work has been published (Kuby et al., 1986).

Experimental Procedures

Materials. Adenylate kinase from rabbit muscle was purified to homogeneity according to Kuby et al. (1978) and crystallized 3 times. The range of specific activities (1094 ± 20 units/mg) was appropriate for the pure enzyme. Adenylate kinase from porcine muscle, purchased from Sigma as an ammonium sulfate suspension, was purified to homogeneity on a Sephadex G-50 column as described by Smith and Mildvan (1982) and was subsequently concentrated by vacuum filtration with Millipore Immersible CX10 concentrators. β,γ-Bidentate Cr^{3+}AMPPCP was prepared according to method B of Dunaway-Mariano and Cleland (1980a), substituting AMPPCP for ATP, as previously described (Granot et al., 1980). AMPPCP, AMP, Tris, and DTT were purchased from Sigma. Chelex 100 (100–200 mesh) and Dowex H^+ 50W-X2 (100–200 mesh) were obtained from Bio-Rad. Sephadex G-25 (medium) was from Pharmacia. Collodion bags (M_r 10 000 cutoff) were from Schleicher & Schuell. D_2O (99.8%), NaOD, and CD_3COOD were from Stohler; D_2O (99.96%) for final deuteriation was obtained from Wilmad.

Sample Preparation. Adenylate kinase from rabbit muscle was stored at −70 °C in 25 mM DTE, 25 mM EDTA, and 20.5% ammonium sulfate. Before use, the enzyme was equilibrated with Tris-HCl, pH 7.2–7.4 (1 mM), KCl (35 mM), and DTT (0.1 mM) by passage through a Sephadex G-25 column. The enzyme was concentrated by vacuum dialysis in collodion bags, and exchangeable protons were deuteriated by two rounds of lyophilization and redissolution into D_2O. Routine activity assays were performed according to the coupled enzyme method, in the direction of ATP production, with hexokinase and glucose-6-phosphate dehydrogenase, as described by Kuby et al. (1978). The concentration of adenylate kinase was determined by its absorbance at 280 nm with $\epsilon = 0.52$ $(mg/mL)^{-1}$ cm^{-1}.

Cr^{3+}AMPPCP was prepared immediately before use. Its concentration was determined by absorbance at 424 and 260 nm. It was deuteriated by repeated D_2O dilution and concentration by high-vacuum rotatory evaporation in a 10 °C water bath. Concentrations of AMPPCP and AMP were determined spectrophotometrically, and these compounds were deuteriated by repeated lyophylization and dissolution in D_2O.

NMR samples contained 1 mM Tris-HCl, 35 mM KCl, 0.1 mM DTT, 7.8–23 mM AMP, and 0.3–1.1 mM adenylate kinase. Solutions were treated with Chelex-100 to remove metal impurities. For experiments involving Cr^{3+}AMPPCP, samples were maintained at pH* 5.6 to ensure the stability of the Cr^{3+} complex. For the NOE experiments, samples were maintained at pH* 7.2. The pH of deuteriated solutions was adjusted with dilute NaOD and CD_3COOD. Samples for phosphorus experiments were 2.0 mL in volume and contained 20% D_2O. Samples for proton NMR were 0.35 mL and fully deuteriated. Control experiments were performed with samples equivalent to those described but without enzyme.

Titration with Cr^{3+}AMPPCP was accomplished by adding small aliquots of a concentrated stock solution directly into the NMR tube, followed by mixing by repeated inversion of the tube. High concentrations of MgAMPPCP needed to displace Cr^{3+}AMPPCP from the enzyme were achieved by dissolving into the NMR sample a lyophilized amount of MgAMPPCP quantitated to produce the desired final concentration.

Kinetic Studies. The inhibition of adenylate kinase by Cr^{3+}AMPPCP with respect to MgATP was studied by the coupled enzyme assay system in the direction of ADP formation, with pyruvate kinase and lactate dehydrogenase (Hamada & Kuby, 1978). The AMP concentration was maintained at a saturating level as described, while MgATP was varied from 15 to 200 μM. Other aspects of the assay were as described, except that the solution was set at pH 5.6, as in the NMR samples, to ensure the stability of the Cr^{3+} complex. Cr^{3+}AMPPCP was added at concentrations of 0–788 μM. Assays were carried out at 25 °C.

NMR Experiments. Proton NMR experiments at 250 MHz and ^{31}P NMR experiments at 101 MHz were performed at 24 °C on a Bruker WM 250 spectrometer using 16-bit A/D conversion for proton NMR and 12-bit A/D conversion for phosphorus. Chemical shifts were determined with reference to external DSS (protons) or H_3PO_4 (phosphorus). Water proton relaxation rates at 24.3 MHz were made on a Semico pulsed NMR spectrometer, at 250 MHz on a Bruker WM 250 spectrometer, and at 360 MHz on a Bruker wide-bore AM 360 spectrometer.

^{31}P spectra were obtained at 101 MHz by collecting 16K data points over a spectral width of 5000 Hz, for an acquisition time of 1.6 s. A 25-s delay was added to obtain fully relaxed spectra. Samples for Cr^{3+}AMPPCP experiments were prepared as described, at [AMP]/[enzyme] ratios of 70/1. T_1 measurements were made by nonselective saturation–recovery. T_2 values were derived from the widths of resonances at half-height ($\Delta\nu_{1/2}$), where $1/T_2 = \pi\Delta\nu_{1/2}$. Spectra were typically acquired by collecting 16 transients.

Proton NMR spectra were obtained at 250 MHz by collecting 16K data points over a spectral width of 2500 Hz, for an acquisition time of 3.3 s. Fully relaxed spectra were obtained by adding an 11.2-s delay between transients. Samples for proton NMR experiments with Cr^{3+}AMPPCP were prepared as described, at [AMP]/[enzyme] ratios of 20/1. T_1 and T_2 measurements were made as described above. Spectra were generally acquired by collecting 16 transients. The dipolar correlation time was determined as previously described (Fry et al., 1985), by the frequency dependence of the paramagnetic effect of the enzyme–Cr^{3+}AMPPCP–AMP complex on $1/T_1$ of water protons at 24.3, 250, and 360 MHz. Since correlation times of enzyme-bound Cr^{3+}–nucleotide complexes are dominated by the electron spin relaxation time of Cr^{3+}, this method is appropriate (Gupta et al., 1976; Mildvan & Gupta, 1978).

NOE experiments were performed as previously described (Fry et al., 1985; Rosevear et al., 1983; Mildvan et al., 1984) at [AMP]/[enzyme] ratios of 8/1. In these experiments, T_1 values were measured by selective saturation–recovery (Tropp & Redfield, 1981). NOEs were generated by alternately preirradiating on and off the resonances of interest, in blocks of 16 transients each, according to the sequence (Fry et al., 1985; Rosevear et al., 1983; Mildvan et al., 1984)

$$[[\text{RD–preirrad}(t,\omega_1)\text{–observe pulse}]_{16}\text{–}[\text{RD–preirrad}(t,\omega_{control})\text{–observe pulse}]_{16}\text{–}[\text{RD–preirrad}(t,\omega_2)\text{–observe pulse}]_{16}]_{8or16}$$

where t is the duration of the preirradiation pulse (0.2–2.0 s), ω_1 and ω_2 are the AMP or enzyme resonances, $\omega_{control}$ is a control frequency (9.7 ppm) far from any resonances, and RD is a relaxation delay of 2.5 s. Preirradiation was performed by using the decoupler at a power of 35 dB below 0.2 W for routine acquisition of NOEs and at 40 dB below 0.2 W for further distinction between primary and secondary effects and for checking the reproducibility and location of intermolecular NOEs. The time dependence of the development of intramolecular NOEs on enzyme-bound AMP was measured by

Table I: Titration of Enzyme-Bound AMP with Cr^{3+}AMPPCP: Effect on ^{31}P Resonance

[enzyme] (μM)	[total Cr^{3+}AMPPCP] (μM)[a]	[bound Cr^{3+}AMPPCP] (μM)[b]	[AMP] (mM)	[total MgAMP-PCP] (mM)[f]	f ($\times 10^4$)[c]	^{31}P resonance of AMP			
						$1/T_1$ (s^{-1})[d]	$1/T_{1P}$ (s^{-1})[e]	$1/T_2$ (s^{-1})[d]	$1/T_{2P}$ (s^{-1})[e]
318	0	0	23.0		0	0.20		5.2	
316	16	7.1	22.9		3.1	0.39	0.19	7.7	2.5
315	41	17.8	22.8		7.8	0.76	0.56	11.9	6.7
313	81	33.8	22.7		14.9	1.22	1.02	13.8	8.6
311	108	44.0	22.6		19.4	1.58	1.38	18.0	13.2
311	108		22.6	26		0.65	0.45	6.3	0.9
311	108		22.6	41		0.65	0.45	6.3	0.9

[a] Titration with Cr^{3+}AMPPCP was performed by adding small aliquots of a concentrated stock solution to the enzyme–AMP sample. [b] Concentrations of bound Cr^{3+}AMPPCP were determined by using its K_i on adenylate kinase (389 μM; Figure 1). [c] f = [bound Cr^{3+}AMPPCP]/[AMP]. [d] T_1 measurements were made with saturation–recovery as described in the text. T_2 values were calculated from line widths of resonances at half-height. Errors in $1/T_1$ and $1/T_2$ measurements are ±10%. [e] $1/T_{1(2)P} = 1/T_{1(2)+Cr^{3+}AMPPCP} - 1/T_{1(2)0Cr^{3+}AMPPCP}$. [f] An excess of MgAMPPCP was used to displace Cr^{3+}AMPPCP from the enzyme.

varying the preirradiation time, over the range 0.2–2.0 s. For experiments in which intermolecular NOEs from the enzyme to AMP were sought, the preirradiation time was set at 0.3 s, and its frequency was advanced through the enzyme spectrum at intervals of 0.1 ppm, over the ranges 0.0–3.7 ppm and 5.8–8.0 ppm downfield from DSS. NOEs were measured by subtracting control spectra ($\omega_{control}$) from experimental spectra (ω_1 and ω_2). NMR experiments were terminated before the enzyme activity dropped below 70%, which was generally ~12 h at pH* 5.6 and ~36 h at pH* 7.2.

Modeling Studies. The conformation of enzyme-bound AMP was studied by building a skeletal model of AMP and adjusting it to accommodate the distances obtained from the NMR experiments. Locating the AMP-binding site within the enzyme was accomplished on an Evans and Sutherland PS300 computer graphics system using the programs MOGLI and FRODO. The X-ray structure of porcine adenylate kinase (Sachsenheimer & Schulz, 1977) was utilized, and AMP was generated in its proper enzyme-bound conformation and fit into the enzyme while the van der Waals surfaces and the intermolecular distance constraints determined by NMR were monitored.

RESULTS

Inhibition of Adenylate Kinase by Cr^{3+}AMPPCP. Cr^{3+}-AMPPCP was chosen as a nonreactive paramagnetic analogue of MgATP for studying intersubstrate distances between enzyme-bound metal–ATP and bound AMP. Cr^{3+}ATP was not used because it would be slowly turned over (Dunaway-Mariano & Cleland, 1980b) during the NMR experiments, which typically required ~10 h to complete. The suitability of Cr^{3+}AMPPCP as an analogue of MgATP was demonstrated in kinetic studies (Figure 1). Cr^{3+}AMPPCP was found to be a linear competitive inhibitor of rabbit muscle adenylate kinase with respect to MgATP, exhibiting a K_I of 389 ± 20 μM. Kinetic experiments with porcine adenylate kinase (data not shown) also revealed linear competitive inhibition by Cr^{3+}AMPPCP with respect to MgATP with a similar K_I of 424 ± 60 μM.

Paramagnetic Effects of Cr^{3+}AMPPCP on the ^{31}P Resonance of Enzyme-Bound AMP. Cr^{3+}AMPPCP was titrated into a solution containing rabbit muscle adenylate kinase and AMP, and the $1/T_1$ and $1/T_2$ values of the ^{31}P resonance of AMP were monitored (Table I). The values of $1/T_1$ (Table I, Figure 2A) and $1/T_2$ (Table I) increased linearly with respect to bound Cr^{3+}AMPPCP. The slopes of such titrations yielded the paramagnetic effects on these relaxation rates.

Displacement of Cr^{3+}AMPPCP from the active site of the enzyme was achieved by the addition of excess MgAMPPCP. Maximal displacement occurred at concentrations of

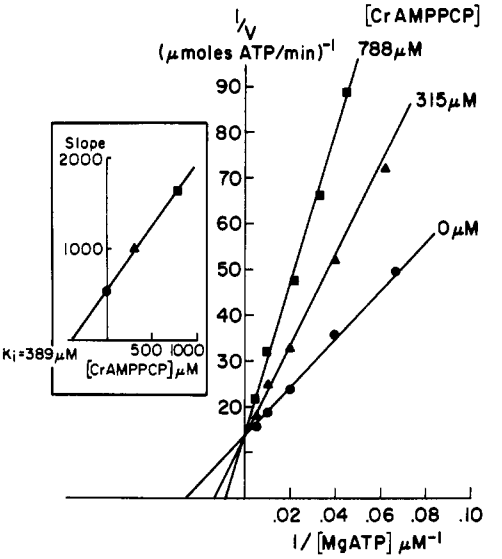

FIGURE 1: Double-reciprocal plot showing inhibition of adenylate kinase by Cr^{3+}AMPPCP. Components present in the coupled assay (Kuby et al., 1978) were AMP (10 mM), K^+-MES buffer, pH 5.6 (50 mM), KCl (35 mM), $MgCl_2$ (8 mM), phosphoenolpyruvate (4.5 mM), NADH (0.2 mM), lactate dehydrogenase (20 units), pyruvate kinase (10 units), and adenylate kinase (0.02γ) in a total volume of 1.0 mL. T = 25 °C.

MgAMPPCP above 26 mM. The K_I of MgAMPPCP on rabbit muscle adenylate kinase, as determined from kinetic experiments (not shown), was ~190 μM. The concentrations of MgAMPPCP used, therefore, should have been adequate to displace all of the bound Cr^{3+}AMPPCP. Small residual paramagnetic effects on $1/T_1$ and $1/T_2$ of the ^{31}P resonance of AMP remained, following the displacement of Cr^{3+}-AMPPCP by MgAMPPCP (Table I), indicating that the enzyme had enhanced the effects of Cr^{3+}AMPPCP on $1/T_1$ and $1/T_2$ by factors of 3.1 and 14.7, respectively. The residual paramagnetic effects, which were comparable in magnitude to those of Cr^{3+}AMPPCP on the relaxation rates of the ^{31}P resonance of AMP observed in control titrations in the absence of enzyme, represent small outer sphere contributions to relaxation (Mildvan & Gupta, 1978; Mildvan et al., 1980).

The paramagnetic effect of Cr^{3+}AMPPCP on $1/T_1$ of the ^{31}P resonance of AMP was derived from a least-squares fit of the graph of $1/T_1$ vs. f, where f = [bound Cr^{3+}-AMPPCP]/[AMP] (Figure 2). The value of $1/T_1$ was adjusted by subtracting the residual outer sphere effect following displacement by MgAMPPCP, yielding a final, corrected $1T_{1P,cor} = 1.37 - 0.45 = 0.92\ s^{-1}$. At this concentration of Cr^{3+}AMPPCP, $f = 19.4 \times 10^{-4}$. Therefore, $1/fT_{1P,cor} = 474 \pm 90\ s^{-1}$. The same method of correction was applied to $1/T_2$,

Table II: Normalized Relaxation Rates and Distances from Cr^{3+}AMPPCP to the Phosphorus and Protons of AMP Bound to Adenylate Kinase

atom	$1/fT_{1P,cor}$ (s^{-1})[a]	$1/fT_{2P,cor}$ (s^{-1})[b]	r (Å)[c]
P	474 ± 90	6340 ± 1100	5.9 ± 0.3
H8	195 ± 41	2160 ± 380	8.9 ± 0.7
H2	228 ± 40	1520 ± 270	8.7 ± 0.6
H1′	106 ± 16	1050 ± 190	9.9 ± 0.7
H3′	299 ± 45		8.3 ± 0.5
H4′	105 ± 20	840 ± 150	9.9 ± 0.7
H5′	374 ± 51	2630 ± 470	8.1 ± 0.5

[a] $1/fT_{1P,cor}$ values were obtained in the following manner: for phosphorus, $1/fT_{1P,cor} = 1/f$ at maximal Cr^{3+}AMPPCP (Table I) × [value of $1/T_{1P}$ at maximal Cr^{3+}AMPPCP from a least-squares fit of $1/T_1$ vs. f (Figure 2) minus $1/T_1$ following displacement with MgAMPPCP (Table I)]; for protons, $1/fT_{1P,cor}$ = slope of graph of $1/T_{1,cor}$ (Table III) vs. f (Figure 2B). [b] $1/fT_{2P,cor}$ = slope of a graph (not shown) of $1/T_{2P,cor}$ vs. f. $1/T_2$ values were calculated as $\pi\Delta\nu_{1/2}$. Complex splitting of the H3′ resonance precluded measurement of its $1/T_2$. [c] Distances (r) between Cr^{3+} and the atoms of AMP were calculated as described in the text. The τ_c was determined as 3.5×10^{-10} s, and the $f(\tau_c)$ values were 1.0×10^{-9} s for phosphorus and 8.1×10^{-10} s for protons. Errors in r include contributions from errors in $1/fT_{1P}$ and τ_c.

yielding $1/fT_{2P,cor} = 6340 \pm 1100$ s^{-1} for rabbit muscle adenylate kinase (Table II).

With porcine adenylate kinase, ^{31}P relaxation measurements of AMP in the ternary enzyme–Cr^{3+}AMPPCP–AMP complex yielded values of $1/fT_{1P,cor} = 508 \pm 60$ s^{-1} and $1/fT_{2P,cor} = 6280 \pm 1000$ s^{-1}, indistinguishable from those found for the rabbit enzyme.

Paramagnetic Effects of Cr^{3+}AMPPCP on the ^1H Resonances of Enzyme-Bound AMP. Experiments examining the paramagnetic effects of Cr^{3+}AMPPCP on the proton resonances of enzyme-bound AMP were performed in a manner analogous to those in which the ^{31}P resonance was observed. Only the enzyme from rabbit muscle was used for these studies. Increases in $1/T_1$ and $1/T_2$ were monitored for the visible proton resonances of AMP, namely, adenine ring protons H8 and H2 and ribose ring protons H1′, H3′, H4′, and H5′. A proton spectrum of a sample containing adenylate kinase and a 20-fold excess of AMP before the addition of Cr^{3+}AMPPCP is shown in Figure 3. The increases in $1/T_1$ (Table III) and $1/T_2$ (not shown) for all six proton resonances were linear with respect to the concentration of bound Cr^{3+}-AMPPCP (Figure 2B).

To provide a correction for the outer sphere contribution to $1/T_1$ and $1/T_2$, a control experiment was performed by titrating comparable amounts of Cr^{3+}AMPPCP into an identical sample of AMP that lacked enzyme, in order to quantitate the effect of unbound Cr^{3+}AMPPCP on the AMP resonances. At each titration level used with the enzyme sample, the concentration of unbound Cr^{3+}AMPPCP was calculated from the K_I and a corresponding $1/T_{1P}$ value for each proton resonance was derived from the control experiment (Table III). This value was subtracted from the observed $1/T_1$ to yield a corrected value, $1/T_{1,cor}$ (Table III, Figure 2B), which reflects the paramagnetic effect of bound Cr^{3+}AMPPCP only.

Displacement of Cr^{3+}AMPPCP following the final titration level (146 μM) was accomplished by adding 44.7 mM MgAMPPCP. The proton resonances of AMP were obscured by those of MgAMPPCP, with the exception of H5′. As expected, the paramagnetic effect on the H5′ resonance was not completely removed following displacement of Cr^{3+}-AMPPCP from the enzyme (Table III). The residual $1/T_{1P}$ (3.57 $s^{-1} - 2.34$ $s^{-1} = 1.23$ s^{-1}) was comparable to that due to unbound Cr^{3+}AMPPCP at the final titration level as de-

Table III: Titration of Enzyme-Bound AMP with Cr^{3+}AMPPCP: Effects on ^1H Resonances

[enzyme] (μM)	[total CrAMPPCP] (μM)[a]	[bound CrAMPPCP] (μM)[b]	[AMP] (mM)	f ($\times 10^4$)[c]	proton resonances of AMP															
					H1′					H3′			H4′			H5′				
					$1/T_1$[d]	$1/T_{1P}$[e]	$1/T_{1,cor}$[f]	$1/T_1$	$1/T_{1P}$	$1/T_{1,cor}$	$1/T_1$	$1/T_{1P}$	$1/T_{1,cor}$	$1/T_1$	$1/T_{1P}$	$1/T_{1,cor}$	$1/T_1$	$1/T_{1P}$	$1/T_{1,cor}$
500	0	0	10		0.88		0.88	0.46		0.46	0.67		0.67	1.03		1.03	1.26		1.26	2.34		2.34
498	16.9	9.4	9.95	9.4	1.35	0.30	1.05	1.00	0.29	0.71	0.80	0.09	0.71	1.47	0.11	1.36	1.28	0.07	1.21	2.94	0.15	2.79
493	50.1	27.3	9.86	27.7	2.33	0.90	1.43	2.08	0.89	1.19	1.19	0.28	0.91	2.13	0.32	1.81	1.52	0.23	1.29	3.70	0.46	3.24
488	82.8	44.1	9.77	45.0	3.51	1.52	1.99	3.17	1.51	1.66	1.49	0.48	1.01	2.74	0.54	2.40	1.82	0.39	1.43	5.00	0.79	4.21
480	146	74.5	9.59	77.5	5.13	2.81	2.32	5.00	2.80	2.20	2.38	0.88	1.50	4.35	0.99	3.36	2.78	0.72	2.06	6.67	1.45	5.22[g]
480[h]	146	0.1	9.59	0.1																3.57[i]		

[a] Titration with Cr^{3+}AMPPCP was performed by adding small aliquots of a concentrated stock solution to the enzyme–AMP sample. [b] Concentrations of bound Cr^{3+}AMPPCP were determined by using its K_I on adenylate kinase (389 μM; Figure 1). [c] f = [bound Cr^{3+}AMPPCP]/[AMP]. [d] T_1 measurements were made by using total saturation–recovery of the proton resonances, as described in the text. Errors in $1/T_1$ are ±10%. All $1/T_1$ values are expressed as s^{-1}. [e] The paramagnetic effect on $1/T_1$ due to unbound Cr^{3+}AMPPCP ($1/T_{1P}$) was determined from a control experiment in which Cr^{3+}AMPPCP was titrated against AMP in an equivalent sample lacking adenylate kinase. At each level of Cr^{3+}AMPPCP addition to the enzyme–AMP sample, the concentration of unbound Cr^{3+}AMPPCP was calculated, and a corresponding $1/T_{1P}$ value was derived from the control experiment. Errors in unbound $1/T_{1P}$ values are ±15%. [f] $1/T_{1,cor}$ = the $1/T_1$ value corrected for effects due to unbound Cr^{3+}AMPPCP ($1/T_{1,cor} = 1/T_{1,obsd}$ − unbound $1/T_{1P}$). Errors in $1/T_{1,cor}$ values are ±18%. [g] A similar value was obtained when $1/T_1$ was corrected for the value found on displacement with MgAMPPCP, i.e., $1/T_{1,cor} = (1/T_{1,max Cr^{3+}AMPPCP} - 1/T_{1,MgAMPPCP}) + 1/T_{1(0)} = 5.44$ s^{-1}, where $1/T_{1(0)}$ represents the relaxation rate prior to the addition of Cr^{3+}AMPPCP. [h] Excess MgAMPPCP (44.7 mM) was added to displace Cr^{3+}AMPPCP from the enzyme. [i] Of the proton resonances of AMP, only that of H5′ remained unobscured by the addition of MgAMPPCP.

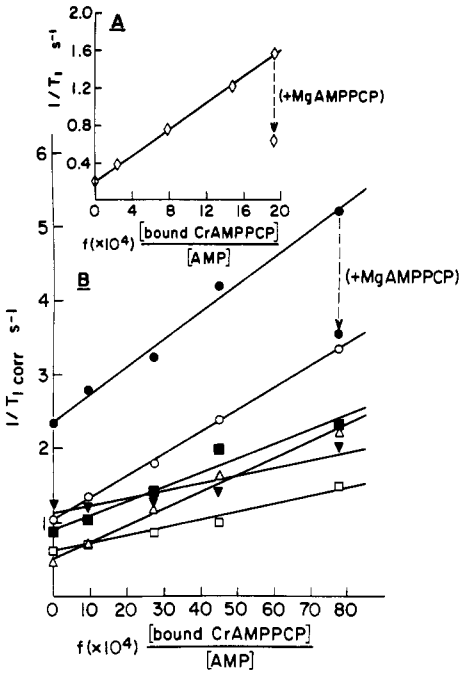

FIGURE 2: Paramagnetic effects of adenylate kinase bound Cr^{3+}-AMPPCP on the phosphorus (A) and proton resonances (B) of AMP. (A) $1/T_1$ of ^{31}P vs. enzyme-bound [Cr^{3+}AMPPCP]/[AMP], showing displacement of Cr^{3+}AMPPCP by 41 mM MgAMPPCP. Components present were adenylate kinase (0.31 mM), AMP (22.6 mM), K-MES, pH 5.6 (50 mM), KCl (35 mM), and D_2O (20%). T = 24 °C; frequency = 101 MHz. Other NMR conditions are given under Materials and Methods. (B) $1/T_1$ of carbon-bound protons of AMP vs. bound [Cr^{3+}AMPPCP]/[AMP], corrected for the outer sphere contribution as described in text. (●) H5′; (○) H3′; (■) H8; (△) H2; (▼) H4′; (□) H1′. Components present were adenylate kinase (0.50 mM), AMP (10 mM), Tris-HCl (1 mM), and KCl (34 mM) in D_2O (100%). Displacement was with 44.7 mM MgAMPPCP. T = 24 °C; frequency = 250 MHz. Other NMR conditions are given under Materials and Methods.

termined in a separate experiment lacking enzyme (1.45 s^{-1}).[2] Values for $1/fT_{1P,cor}$, the normalized, corrected paramagnetic effect of enzyme-bound Cr^{3+}AMPPCP on the longitudinal relaxation rates of each proton of AMP, were obtained from the slopes of Figure 2B and are given in Table II.

$1/T_2$ values were corrected for the effects of unbound Cr^{3+}AMPPCP in a manner analogous to $1/T_1$. Values for $1/fT_{2P,cor}$ were obtained from slopes of graphs of $1/T_{2,cor}$ vs. f (not shown) and are given in Table II. The residual $1/T_{2P}$ for H5′ following displacement of Cr^{3+}AMPPCP by MgAMPPCP (1.5 s^{-1}) was comparable to that due to unbound Cr^{3+}AMPPCP at the final titration level as determined in absence of enzyme (1.7 s^{-1}).[2]

Kinetic Properties of the Enzyme–Cr^{3+}AMPPCP–AMP Complex. A lower limit to the rate constant for dissociation (k_{off}) of AMP from the ternary enzyme–Cr^{3+}AMPPCP–AMP complex of 6340 s^{-1} may be estimated from the largest $1/fT_{2P,cor}$ value of rabbit muscle adenylate kinase (Table II) (Mildvan & Gupta, 1978). This value exceeds k_{cat} of the adenylate kinase reaction in the direction of AMP formation (464 s^{-1}) by an order of magnitude, consistent with a rapid equilibrium random kinetic scheme in both directions as found by kinetic studies (Hamada & Kuby, 1978). Thus, the ternary complex studied by NMR has kinetic properties similar to that of the active ternary complex. The lower limit of the k_{off} value of AMP, together with the dissociation constant of AMP from the active ternary complex (94 ± 10 μM; Hamada & Kuby, 1978), yields a lower limit to the rate constant for AMP binding, $k_{on} \geq 6.7 \times 10^7$ M^{-1} s^{-1}, which is below the diffusion limit. The identical value of the $1/fT_{2P,cor}$ of the phosphorus of AMP found with the porcine adenylate kinase–Cr^{3+}-AMPPCP–AMP complex suggests similar exchange properties of AMP on this enzyme as well.

Calculation of Distances from Cr^{3+}AMPPCP to ^1H and ^{31}P Resonances of Bound AMP. Distances may be calculated from the paramagnetic effects of Cr^{3+} on $1/T_1$ of nearby enzyme-bound nuclei, providing that this effect ($1/fT_{1P,cor}$) is not limited by the rate of exchange of the substrate on and off the enzyme (Mildvan et al., 1980). The lower limit to the exchange rate of AMP, as derived from the maximum $1/fT_{2,cor}$ measurement, 6340 s^{-1}, is at least an order of magnitude greater than any of the measured $1/fT_{1P,cor}$ values (Table II). Therefore, the $1/fT_{1P,cor}$ values may be used to calculate distances with (Mildvan & Gupta, 1978; Mildvan et al., 1980)

$$r = C[fT_{1P,cor}f(\tau_c)]^{1/6} \quad (1)$$

$$f(\tau_c) = \frac{3\tau_c}{1 + \omega_I^2\tau_c^2} + \frac{7\tau_c}{1 + \omega_S^2\tau_c^2} \quad (2)$$

where C is a constant equal to 705 Å/$s^{1/3}$ for Cr^{3+}–proton interactions and 522 Å/$s^{1/3}$ for Cr^{3+}–phosphorus interactions, τ_c is the dipolar correlation time, and ω_I and ω_S are the nuclear and electron precession frequencies.

For the ternary rabbit muscle adenylate kinase–Cr^{3+}-AMPPCP–AMP complex, the dipolar correlation time was found to be (3.5 ± 0.4) × 10^{-10} s at 250 MHz, as determined by the frequency dependence of $(1/T_{1P})_b$ of water protons due to enzyme-bound Cr^{3+}AMPPCP at 24.3, 250, and 360 MHz. The correlation time was calculated with the equations of the Solomon–Bloembergen–Morgan theory (Mildvan & Gupta, 1978). The value of the correlation time is comparable to that found for the binary adenylate kinase–Cr^{3+}ATP complex [(6.2 ± 1.2) × 10^{-10} s; Smith & Mildvan, 1983] and represents a typical electron spin relaxation time of Cr^{3+} (Cleland & Mildvan, 1979). From this value, $f(\tau_c)$ is calculated as 8.1 × 10^{-10} s for protons and 1.0 × 10^{-9} s for phosphorus (eq 2). Insertion of the measured $fT_{1P,cor}$ values and appropriate $f(\tau_c)$ values into eq 1 yielded distances between the Cr^{3+} atom of Cr^{3+}AMPPCP and the six protons and the phosphorus atom of AMP on rabbit muscle adenylate kinase (Table II). The distance from Cr^{3+} to phosphorus obtained with the rabbit enzyme (5.9 ± 0.3 Å, Table II) probably also applies to porcine adenylate kinase since the $1/fT_{1P,cor}$ values were equal, assuming the correlation time for the two enzymes to be the same. This distance overlaps with the results of a single distance measurement from Cr^{3+}ATP to the phosphorus of AMP on commercial porcine adenylate kinase (6.6 ± 0.6 Å; Gupta, 1980).

Intramolecular Nuclear Overhauser Effects in Enzyme-Bound AMP. Intramolecular NOEs between pairs of protons of AMP bound to rabbit muscle adenylate kinase were negative, as exemplified in Figure 4. These effects were measured by selectively preirradiating the H1′, H2′, H3′, H4′, H5′, and H8 resonances and observing decreases in the magnetizations of the nonirradiated resonances, which were well resolved from those of the enzyme (H1′, H2, and H8). The preirradiation time was varied from 0.2 to 2.0 s in order to obtain the time course of the development of the NOEs, as illustrated in Figure 5.

[2] The slightly reduced values of the residual relaxation rates observed after displacement may be due to the aggregation of Cr^{3+}AMPPCP in the presence of a large excess of MgAMPPCP. The uncertainties in the distances (~3%) resulting from these small uncertainties in the outer sphere contribution to $1/T_{1P}$ are within the experimental errors in the distances (Table II).

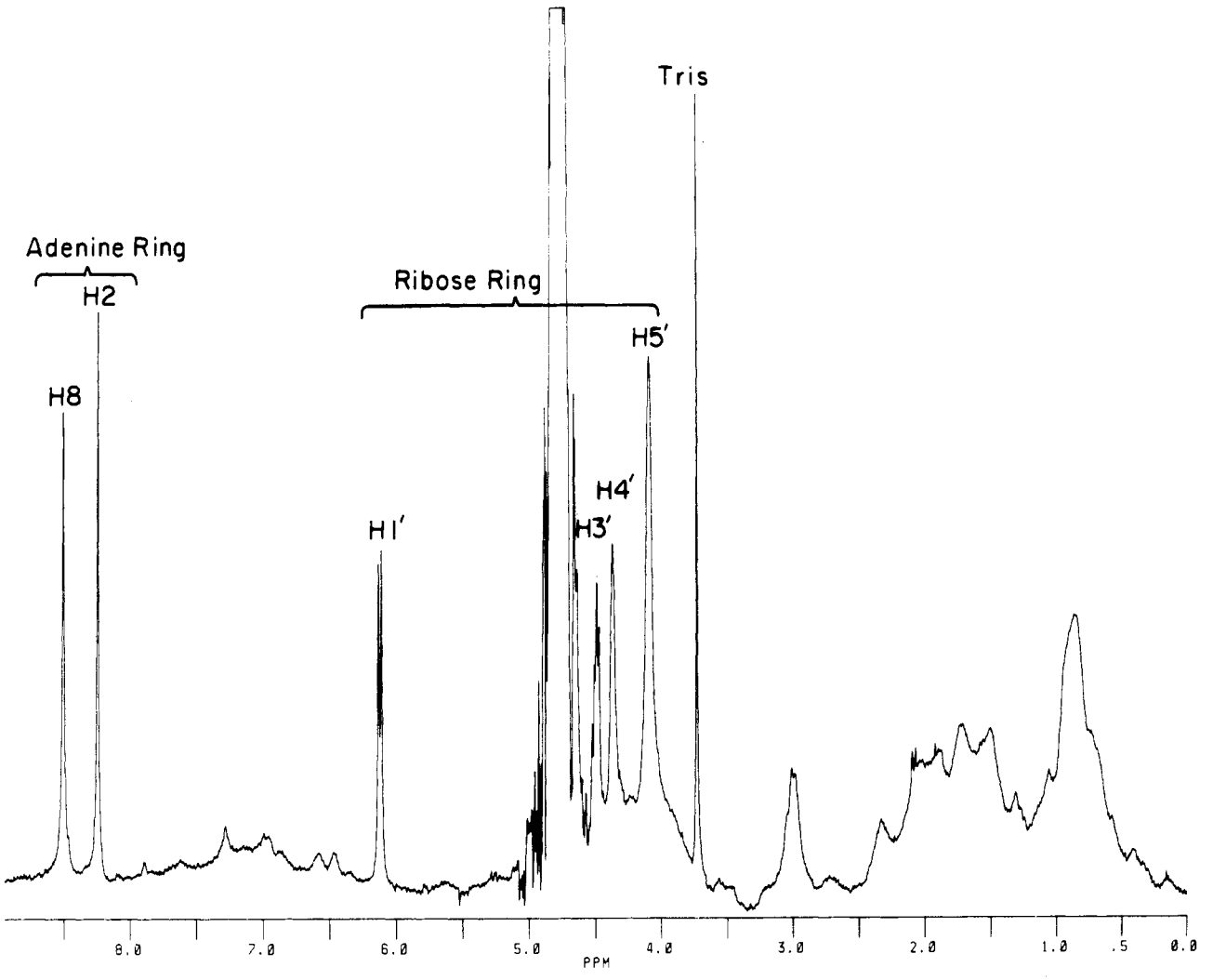

FIGURE 3: Proton NMR spectrum of adenylate kinase and AMP used for Cr^{3+}AMPPCP titration. Components and conditions are as described in Figure 2B.

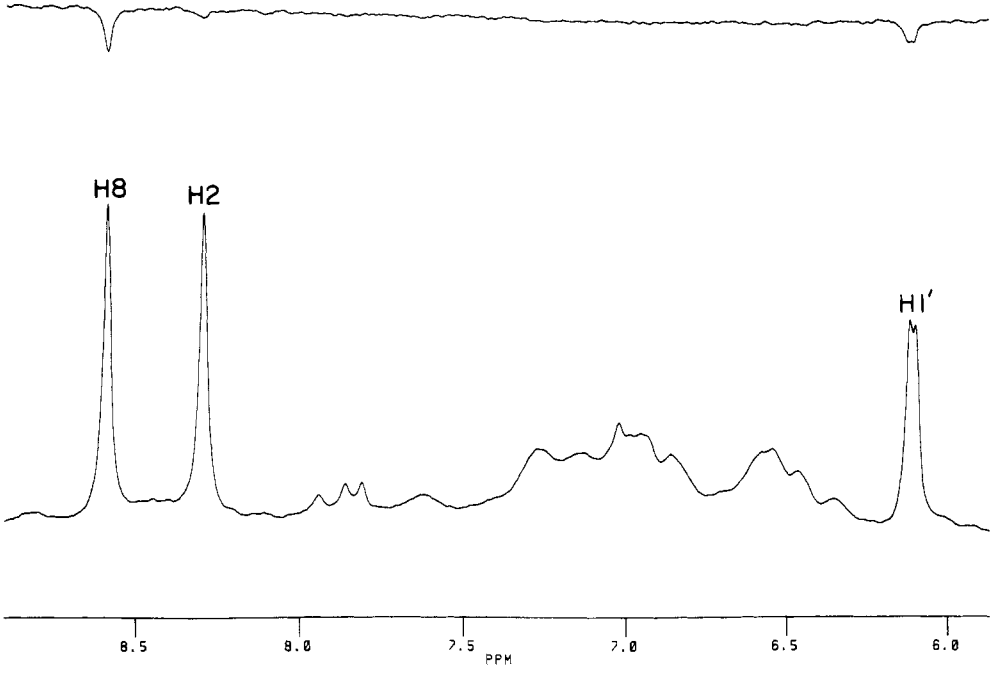

FIGURE 4: Intramolecular nuclear Overhauser effect in AMP bound to adenylate kinase. Shown are the spectra of AMP (7.8 mM) and adenylate kinase (1.1 mM). The upper spectrum is the difference spectrum observed after preirradiation of H2′ of AMP minus that obtained on preirradiation at 9.7 ppm for 1.0 s. Other components present were Tris-HCl, pH* 7.2 (1 mM), KCl (35 mM), and dithiothreitol (0.1 mM). T = 24 °C; frequency = 250 MHz. Other NMR conditions are given under Materials and Methods.

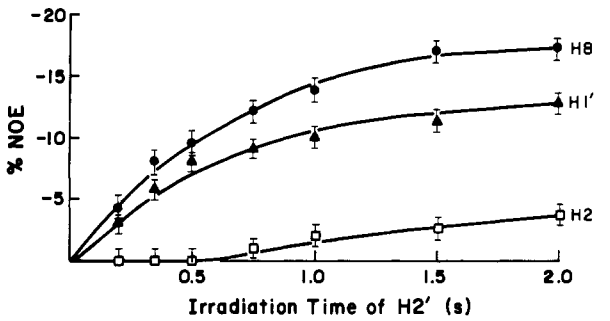

FIGURE 5: Time dependence of the intramolecular nuclear Overhauser effects observed in enzyme-bound AMP. The solid curves through the data points for H8 and H1′ are computed according to eq 3 with the parameters in Table IV. The effect on H2 is secondary. Components and conditions are as described in Figure 4.

Table IV: Intramolecular NOEs and Interproton Distances within AMP Bound to Adenylate Kinase

NOE[a]	σ[b]	r (Å)[c]
H2′–H1′	−0.210	2.70
H2′–H8	−0.285	2.57
H3′–H8	−0.310	2.53
H5′–H8	−0.120	2.96
H4′–H1′	≥−0.070[d]	≥3.24
H1′–H8	≥−0.043	≥3.52
H8–H1′	≥−0.039	≥3.57

[a] NOEs were obtained as described in the text. Effects on H2 were either not observed or shown to be secondary effects due to late appearance (≥0.75 s). [b] Obtained from the time dependence of NOE development with eq 3 and the ρ values of H1′ (1.6 ± 0.2 s^{-1}), H2′ (0.87 ± 0.10 s^{-1}), and H8 (1.6 ± 0.2 s^{-1}) independently measured by selective saturation. Errors in σ are ±20%. [c] Obtained with eq 4 with $f(\tau_r) = -1.4 \times 10^{-9}$ as calculated by setting the H2′–H1′ distance at 2.70 Å as a standard. Errors in r are ±8%. [d] For small or unobserved effects, σ was calculated as a lower limit by considering maximal NOEs possible within the noise level of the data.

The cross-relaxation rates (σ) between pairs of protons were determined by fitting the time dependence of the NOEs to (Wagner & Wüthrich, 1979)

$$f_A(B)_t = \frac{\sigma_{AB}}{\rho_A}(1 - e^{-\rho_A t}) + \frac{\sigma_{AB}}{\rho_A - c}(e^{-\rho_A t} - e^{-ct}) \quad (3)$$

where $f_A(B)_t$ is the fractional change in the magnetization of resonance A upon preirradiation of resonance B for t seconds, ρ_A is the longitudinal relaxation rate of resonance A obtained by selective saturation, and c is a rate constant describing the saturation of resonance B. By utilizing measured values for $f_A(B)_t$ and ρ_A and allowing c to vary, best-fit values for σ_{AB} were obtained for each pair of protons (Table IV). For proton pairs that were structurally capable of producing NOEs but did not, a lower limit value for σ is given on the basis of the largest possible NOE that might be present within the noise level of the data. NOEs to H2 were secondary effects, which only appeared at preirradiation times ≥0.75 s.

Cross-relaxation rates were used to determine distances between pairs of protons from

$$r_{AB} = \left[\left(\frac{\gamma^4\hbar^2}{10}\right)(\sigma_{AB})^{-1}\left(\frac{6\tau_r}{1 + 4\omega_1^2\tau_r^2} - \tau_r\right)\right]^{1/6} \quad (4)$$

The rotational correlation time (τ_r) was evaluated by setting the H2′–H1′ distance at 2.70 Å for reasons to be explained below. Using this value and $\sigma_{H2'-H1'}$ in eq 4 yielded a value for τ_r of 1.75×10^{-9} s. This value, which agrees with that found for the H2′–H1′ interactions in MgATP bound to adenylate kinase (1.7×10^{-9} s; Fry et al., 1985), was then used in conjunction with each of the other σ values to determine distances (or lower limit distances) between pairs of protons of AMP (Table IV). In a fast-exchanging enzyme–substrate system, distances derived from intramolecular substrate NOEs reflect those present on the enzyme-bound substrate, reflecting its conformation (Bothner-By, 1979; Rosevear et al., 1983; Fry et al., 1985). This explains why such NOEs were negative for adenylate kinase bound AMP, whereas analogous NOEs are positive on free AMP in the absence of enzyme (data not shown) due to its much lower molecular weight and shorter τ_r as compared to that of the enzyme–substrate complex.

Conformation of AMP Bound to Rabbit Muscle Adenylate Kinase. The collected distance information obtained from the NMR experiments on enzyme-bound AMP (Tables II and IV) was used to determine its conformation. Application of the distance constraints from Cr^{3+}ATP obtained by the paramagnetic probe studies alone (Table II) restricted the conformation of AMP but produced six structures consistent with these constraints, possessing different combinations of sugar puckers (δ), glycosyl torsional angles (χ), and rotations about the C4′–C5′ bond (γ). It has been shown in similar cases (Rosevear et al., 1983) that interproton distances from NOE experiments can help select one structure from such a set of possibilities. However, these distances must be calibrated by use of a standard distance within the system (unless τ_r is directly determined from the frequency dependence of σ (Fry et al., 1985)). For nucleotides such as AMP, the H2′–H1′ distance provides a suitable standard, which lies within the range 2.9 ± 0.2 Å regardless of sugar pucker (Rosevear et al., 1983). In the present case, it was found that setting this distance to 2.70 Å yielded a set of NOE-determined interproton distances (Table IV) that best accommodated the Cr^{3+} to AMP distances obtained from the paramagnetic probe experiments (Table II). A single conformation for enzyme-bound AMP was thereby found which was consistent with all of the distance constraints (Figure 6A). This AMP conformation exhibits a high *anti*-glycosyl torsional angle (χ = 110 ± 10°), a 3′-endo,2′-exo ribose pucker (δ = 105 ± 10°), a gauche,trans orientation about the C4′–C5′ bond (γ = 180 ± 10°), and a gauche,trans orientation about the C5′–O5′ bond (β = 170 ± 20°) (Figure 6B).

The presence of 0.7 mM MgAMPPCP, an amount stoichiometric with enzyme, did not significantly alter the interproton cross-relaxation rates (σ) of AMP, indicating no detectable change in the conformation of enzyme-bound AMP in response to the binding of the metal–ATP analogue.

Intermolecular NOEs between Protons of Adenylate Kinase and Those of Bound AMP. NOEs between protons of rabbit muscle adenylate kinase and those of bound AMP were sought by preirradiating enzyme resonances at 0.1 ppm intervals along the spectrum and looking for effects on the H1′, H2, and H8 proton resonances of AMP. Nine such negative intermolecular NOEs of significant magnitude (<−1%) were observed which were consistently reproducible (Table V). Their chemical shifts indicate that they arise from at least three hydrophobic amino acids in proximity to the adenine–ribose portion of bound AMP. Intermolecular NOEs from similar regions of porcine adenylate kinase, at 1.1, 1.3, and 1.7 ppm, to H2 and H8 of AMP have previously been found (Smith & Mildvan, 1982), indicating very similar binding sites for AMP on the two enzymes.

Discussion

AMP is held at the active site of rabbit muscle adenylate kinase in a single, somewhat unusual conformation. The unusual feature is the combination of a high *anti*-glycosyl torsional angle (χ = 110 ± 10°) with a 3′-endo,2′-exo ribose

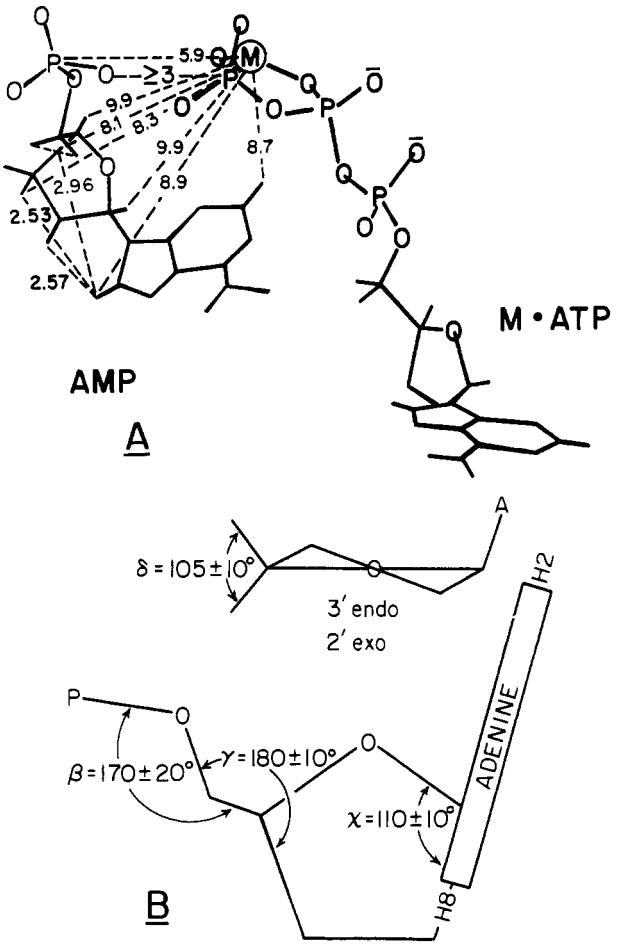

FIGURE 6: Conformations and arrangement of substrates bound to adenylate kinase. (A) Conformation of metal–ATP (Fry et al., 1985) and of AMP showing intersubstrate distances (Table II) and interproton distances (Table IV) in angstrom units. Also shown is the lower limit reaction coordinate distance (≥3 Å) between the entering oxygen of AMP and the γ-phosphorus of metal–ATP determined by model building. (B) Detailed conformation of adenylate kinase bound AMP showing the four conformational angles χ, β, γ, and δ. The glycosidic angle χ is defined by O4′–C1′–N9–C8 (Sundaralingam, 1969), and β is defined by P–O5′–C5′–C4′, γ by O5′–C5′–C4′–C3′, and δ by C5′–C4′–C3′–O3′ (IUPAC–IUB Joint Commission on Biochemical Nomenclature, 1983).

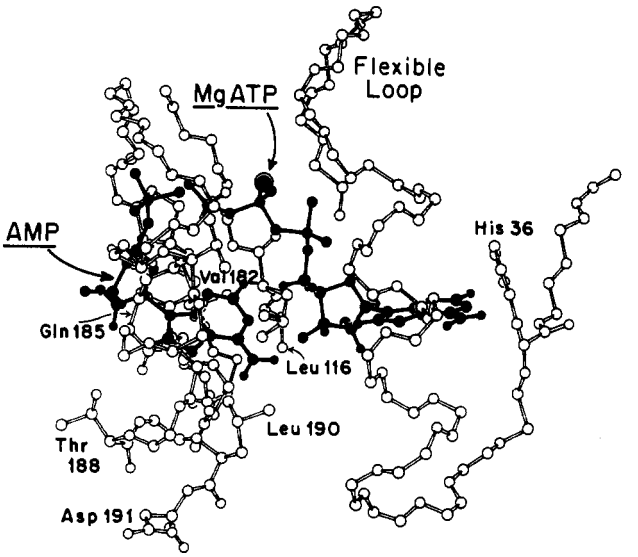

FIGURE 7: ORTEP showing binding sites for AMP and MgATP on adenylate kinase as determined by "NMR docking". The MgATP binding site was previously determined as described by Fry et al. (1985). The AMP site was also located with the Evans and Sutherland PS 300 computer graphics system, on the basis of the conformation of enzyme-bound AMP (Figure 6), the intersubstrate distances (Table II, Figure 6A), and the intermolecular nuclear Overhauser effects from protons of the enzyme to those of AMP (Table V).

pucker. In crystal structures of "high-anti" purine nucleotides, large χ angles ≥70° are usually accompanied by 2′-endo ribose puckers (deLeeuw et al., 1980). Theoretical calculations of the conformational energies of purine ribonucleotides, with both hard sphere (Yathindra & Sundaralingam, 1973) and quantum mechanical methods (Saran et al., 1973), suggest that the conformation of enzyme-bound AMP is higher in energy, by 0.6–1.6 kcal/mol, above the most stable minimum. Hence, the conformation of AMP at the active site of adenylate kinase must be considered somewhat distorted or strained. Such distortion has also been detected by NMR and X-ray in nucleotide substrates bound to other enzymes including DNA polymerase (Sloan et al., 1975; Ferrin & Mildvan, 1985), protein kinase (Rosevear et al., 1983), and hexokinase (Steitz et al., 1981) and correlates with the high nucleotide base specificities of these enzymes (Mildvan, 1981).

The finding of an anti conformation for AMP bound to adenylate kinase is in agreement with the ability of the enzyme to utilize 8,5′-cycloadenosine 5′-phosphate as a substrate (Hampton et al., 1972). Glycosyl torsional angles in the anti range are usually found for nucleotides bound to proteins, including AMP on lactate dehydrogenase (χ = 89°) (Chandrasekhar et al., 1973), the adenosine moiety of NAD on lactate dehydrogenase (χ = 84°) (Chandrasekhar et al., 1973), and MgATP on protein kinase (χ = 78°) (Rosevear et al., 1983) and adenylate kinase (χ = 65°) (Fry et al., 1985).

The torsional angle determined by the rotation about the C4′–C5′ bond (γ) found for AMP on adenylate kinase (180 ± 10°) has also been commonly found in X-ray studies of other ribonucleotides with 3′-endo sugar puckers and *anti*-glycosyl torsional angles (deLeeuw et al., 1980) and is similar to that of AMP bound to lactate dehydrogenase (γ = 178°) (Chandrasekhar et al., 1973) and of MgATP bound to adenylate kinase (γ = 170°) (Fry et al., 1985).

The C4′–C5′–O5′–P torsional angle found for enzyme-bound AMP (β = 170 ± 20°) is within the range (180 ± 30°) that is almost exclusively observed on X-ray studies of mono- and polynucleotides (deLeeuw et al., 1980) and is similar to the values for β observed on nucleotides bound to dehydrogenases (Chandrasekhar et al., 1973; Matthews et al., 1979) and for MgATP bound to adenylate kinase (Fry et al., 1985). Hence, the strain in the conformation of bound AMP is limited to the adenine ribose portion. A limited number of experiments with porcine muscle adenylate kinase reveal no significant differences from the rabbit muscle enzyme with respect to the interactions of Cr^{3+}AMPPCP and AMP.

The proper conformation of enzyme-bound AMP, together with its seven measured distances from bound Cr^{3+}AMPPCP (Table II) and its nine proximities to amino acid proton resonances of the enzyme (Table VI), permitted AMP to be positioned into the X-ray structure of the enzyme, with the Evans and Sutherland computer graphics system. Since Cr^{3+}AMPPCP and Cr^{3+}ATP are both competitive inhibitors with respect to MgATP and Cr^{3+}ATP has substrate activity (Dunaway-Mariano & Cleland, 1980b), the reasonable assumption was made that the Cr^{3+} atom of Cr^{3+}AMPPCP occupies the same position on the enzyme as that previously found for the Cr^{3+} atom of Cr^{3+}ATP (Fry et al., 1985).

AMP, fixed in its bound conformation, was systematically rotated about the previously located Cr^{3+} atom of bound Cr^{3+}ATP in accord with the measured intersubstrate distances, describing a sphere around the Cr^{3+} the surface of which

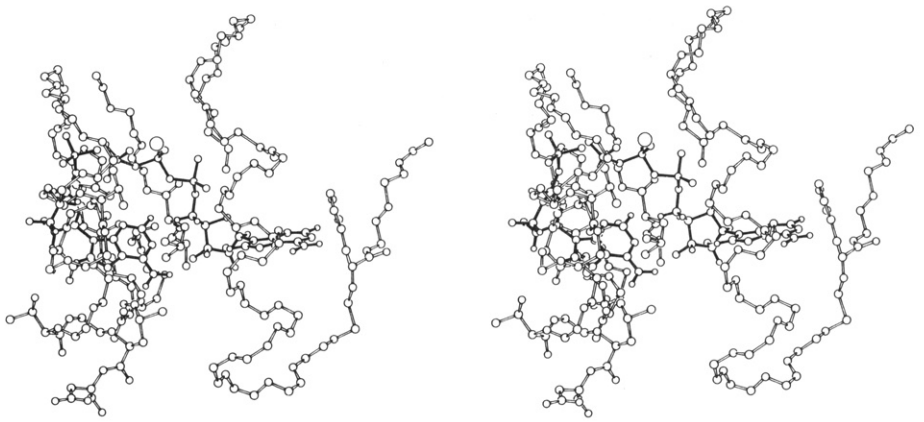

FIGURE 8: ORTEP stereopair showing details of the AMP and MgATP binding sites of adenylate kinase determined by NMR docking.

Table V: Intermolecular NOEs from Resonances of Adenylate Kinase to Those of Bound AMP

NOE from enzyme[a]		to (AMP resonance)	possible identity[c]	assignments and distances (Å)[d]
ppm[b]	% NOE			
1.1	−2.0	H8	CH_3 of L, V, I, T; CH_2 of I	L-190 δ-CH_3 (4.78, 6.67) or V-182 γ-CH_3 (8.72, 9.51)
1.8	−2.0	H8	CH_2 of L, K, R, P; CH of L, I	L-190 γ-CH (5.65)
0.6	−1.8	H2	CH_3 of L, V, I	L-116 δ-CH_3 (1.87, 3.37)
1.1	−3.0	H2	CH_3 of L, V, I, T; CH_2 of I	V-173 γ-CH_3 (3.12, 5.12)
1.4	−4.3	H2	CH_3 of A, T; CH_2 of I, L, K; CH of L	L-116 β-CH_2 (2.84)
1.7	−5.2	H2	CH_2 of L, K, R; CH of L, I	L-116 γ-CH (2.90)
2.1	−1.4	H2	CH_3 of M; CH_2 of E, Q, R, K, P; CH of V, I	R-171 γ-CH_2 (5.44)
1.1	−4.5	H1′	CH_3 of L, V, I, T; CH_2 of I	V-173 γ-CH_3 (3.08, 4.61)
2.3	−2.3	H1′	CH_3 of M; CH_2 of E, Q, R, K, P; CH of V	V-173 β-CH (2.89)

[a] NOEs were sought by irradiating the enzyme resonances at 0.1 ppm intervals, as described in the text. The NOEs listed represent reproducible effects of significant magnitude (<−1%). [b] Chemical shifts are from DSS; the sample was at pH* 7.2. [c] Possible identity of enzyme resonances are based on chemical shifts, from data on model peptides (Wüthrich, 1976; Bundi & Wüthrich, 1979). [d] Assignments and distances (±2 Å) are based upon the AMP-binding site determined from fitting procedures on the computer graphics system, as described under Discussion. Our second best fit placed adenine H8 of AMP 8.50 Å from L-190 δ-CH_3 and 8.43 Å from L-190 γ-CH, and adenine H2 7.28 Å from R-171 γ-CH_3, distances which are inconsistent with the observed NOEs.

represented all possible sites for bound AMP. A location for AMP was sought in which all of the amino acid proximities to AMP detected by the NOE method were satisfied and where atoms of AMP did not overlap with those of the enzyme. Approximately 30% of the sphere of potential sites placed AMP beyond significant contact with the enzyme (above and in front of MgATP in Figure 9). Another 10% caused overlap between AMP and CrATP. Potential binding locations in the

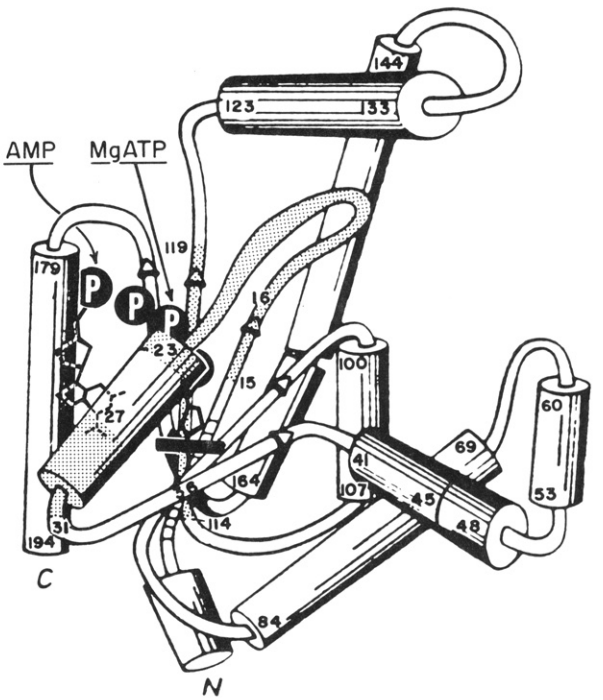

FIGURE 9: Simplified representation of the crystal structure of the entire adenylate kinase molecule showing the location of bound AMP and MgATP as determined by NMR docking. The stippling shows regions of amino acid sequence homology with other nucleotide binding enzymes (Fry et al., 1985).

remaining portion of the sphere were eliminated due to overlap between AMP and the following regions of the enzyme: β-strands 115–120 and 168–173 (behind MgATP, in Figure 9), helix 26–30 (front left of MgATP), helix 180–186 (direct left of MgATP), and loop 15–21 (right of MgATP). The only site found for AMP that avoided significant overlaps and permitted proximities to the correct enzyme side chains for explanation of the observed NOEs is shown in Figures 7–9. The uncertainty of ±2 Å in the position of Cr^{3+} (Fry et al., 1985) introduces a corresponding error in the position of AMP with respect to the enzyme.

The multiple interactions between AMP and the enzyme at this site are consistent with the extremely high specificity of adenylate kinase for AMP. The only known alternative substrates are 2′-dAMP and 8,5′-cycloadenosine 5′-phosphate (Criss et al., 1970; Hampton et al., 1972). As shown in Figures 7–9, the AMP binding site, which is near Leu-116, Arg-171, Val-173, Val-182, and Leu-190, consists in part of the last 23 amino acid residues of adenylate kinase. A peptide based on these residues has been shown to bind ϵAMP (Hamada et al.,

1979), and the rate of chemical modification of Cys-187 is enhanced by AMP but is unaffected by MgATP (Price et al., 1975). Preliminary NMR studies[3] indicate that this peptide shortens the T_1 and T_2 values of the adenine H2 and H8 and the ribose H1′ protons of AMP, consistent with the formation of a peptide–AMP complex. However, NOE studies suggest at least two conformations for peptide-bound AMP, probably due to the incompleteness of the AMP binding site. Further studies with larger peptides from this region of the enzyme are in progress to better approximate the AMP-binding site of the enzyme. Finally, it is of interest to note that residues Leu-116, Arg-171, Val-173, Val-182, and Leu-190 are invariant in muscle-type rabbit, calf, human, porcine (Kuby et al., 1984), and chicken adenylate kinase (Kishi et al., 1986).

An examination of the substrate binding sites with reference to the complete enzyme (Figure 9), together with the detection of a rapid equilibrium random kinetic scheme (Hamada & Kuby, 1978), suggests that the optimum binding pathway differs for the two substrates. In the view shown in Figure 9, MgATP probably enters the active site from the right, while AMP would most easily enter from the left. If this were the case, then the potent inhibition of muscle-type adenylate kinase by the combined substrate analogue Ap_5A (Lienhard & Secemskii, 1973; Kuby et al., 1978) would probably require a conformational change of the enzyme. A change in enzyme conformation has been detected by X-ray analysis upon binding of MnATP (Pai et al., 1977; Sachsenheimer & Schulz, 1977), deduced kinetically (Hamada & Kuby, 1978), and observed by ^{1}H NMR of the human muscle enzyme upon binding of Ap_5A (Kalbitzer et al., 1982).

These results also provide valuable information on the detailed mechanism of the adenylate kinase reaction. As discussed elsewhere (Mildvan & Fry, 1987), the coordination of the γ-phosphate of ATP by the divalent cation and the proximity of Lys-27 to the γ-phosphate on this enzyme suggest an associative nucleophilic substitution on the γ-phosphorus but do not establish such a mechanism. A powerful criterion of mechanism is the reaction coordinate distance (Mildvan, 1981), in this case between the entering oxygen of AMP and the γ-phosphorus of bound metal–ATP. A lower limit to this distance of ≥3 Å is derived from the measured intersubstrate distances (Table II). From our position of enzyme-bound AMP with respect to bound Cr^{3+}AMPPCP, this lower limit distance becomes an actual distance estimated as 3 ± 1 Å. The large error in this derived distance results from the errors in the measured distances, in the positions of the bound substrates, and in the orientation of the P–O bond of AMP. The reaction coordinate distance of 3 ± 1 Å so obtained strongly supports an associative mechanism for adenylate kinase, since there is no room for a metaphosphate intermediate in a dissociative mechanism. A reaction coordinate distance exceeding 4.9 Å is necessary to allow a metaphosphate intermediate, with no bonding to either the leaving or the entering groups, in a fully dissociative mechanism (Mildvan, 1981).

Evidence for a short reaction coordinate distance on a kinase may also be provided kinetically, by cross-product competitive inhibition between the phosphorylated product and MgATP (Mildvan & Fry, 1987). However, such inhibition of adenylate kinase by ADP might also result from direct competition for the MgATP site, rendering the interpretation ambiguous. With the related adenylate kinase from beef heart mitochondria, which utilizes MgGTP to phosphorylate AMP, each binding at highly specific sites, competition of the phosphorylated product ADP with MgGTP has been detected kinetically, providing qualitative evidence for a short reaction coordinate distance and an associative mechanism (Tomasselli & Noda, 1979).

[3] D. C. Fry, S. A. Kuby, and A. S. Mildvan, unpublished observations, 1986.

ACKNOWLEDGMENTS

We are grateful to Engin H. Serpersu and V. P. Chacko for help in T_1 studies of water protons and to Eric Suchanek and Athan Kuliopoulos for assistance with the computer graphics system.

REFERENCES

Bothner-By, A. (1979) in *Biological Applications of Magnetic Resonance* (Shulman, R. G., Ed.) pp 177–219, Academic, New York.

Chandrasekhar, K., McPherson, A., Adams, M. J., & Rossman, M. G. (1973) *J. Mol. Biol. 76*, 503–519.

Cleland, W. W., & Mildvan, A. S. (1979) *Adv. Inorg. Biochem. 1*, 163–191.

Criss, W. E., Sapica, V., & Litwack, G. (1970) *J. Biol. Chem. 245*, 6346–6351.

deLeeuw, H. P. M., Haasnoot, A. C., & Altona, C. (1980) *Isr. J. Chem. 20*, 108–126.

Dunaway-Mariano, D., & Cleland, W. W. (1980a) *Biochemistry 19*, 1496–1505.

Dunaway-Mariano, D., & Cleland, W. W. (1980b) *Biochemistry 19*, 1506–1515.

Ferrin, L. J., & Mildvan, A. S. (1985) *Biochemistry 24*, 6904–6913.

Fry, D. C., Kuby, S. A., & Mildvan, A. S. (1985) *Biochemistry 24*, 4680–4694.

Granot, J., Mildvan, A. S., Bramson, H. N., & Kaiser, E. T. (1980) *Biochemistry 19*, 3537–3543.

Gupta, R. K. (1980) *Biophys. J. 32*, 225–228 (Abstr.).

Gupta, R. K., Fung, C. H., & Mildvan, A. S. (1976) *J. Biol. Chem. 251*, 2421–2430.

Hamada, M., & Kuby, S. A. (1978) *Arch. Biochem. Biophys. 190*, 772–792.

Hamada, M., Palmieri, R. H., Russell, G. A., & Kuby, S. A. (1979) *Arch. Biochem. Biophys. 195*, 155–177.

Hampton, A., Harper, P. J., & Sasaki, T. (1972) *Biochemistry 11*, 4965–4969.

IUPAC–IUB Joint Commission on Biochemical Nomenclature (1983) *Eur. J. Biochem. 131*, 9–15.

Kalbitzer, H. R., Marquetant, R., Rosch, P., & Schirmer, R. H. (1982) *Eur. J. Biochem. 126*, 531–536.

Kishi, F., Maruyama, M., Tanizawa, Y., & Nakazawa, A. (1986) *J. Biol. Chem. 261*, 2942–2945.

Kuby, S. A., Hamada, M., Gerber, D., Tsai, W. C., Jacobs, H. K., Cress, M. C., Chua, S. K., Fleming, G., Wu, L. H., Fischer, A. H., Frischat, A., & Maland, L. (1978) *Arch. Biochem. Biophys. 187*, 34–52.

Kuby, S. A., Palmieri, R. H., Frischat, A., Fischer, A. H., Wu, L. H., Maland, L., & Manship, M. (1984) *Biochemistry 23*, 2393–2399.

Kuby, S. A., Fry, D. C., & Mildvan, A. S. (1986) *Fed. Proc., Fed. Am. Soc. Exp. Biol. 45*, 1647.

Lienhard, G. E., & Secemski, I. I. (1973) *J. Biol. Chem. 248*, 1121–1123.

Mildvan, A. S. (1981) *Philos. Trans. R. Soc. London, B 293*, 65–74.

Mildvan, A. S., & Gupta, R. K. (1978) *Methods Enzymol. 49G*, 322–359.

Mildvan, A. S., & Fry, D. C. (1987) *Adv. Enzymol. Relat. Areas Mol. Biol. 59*, 241–313.

Mildvan, A. S., Granot, J., Smith, G. M., & Liebman, M. N. (1980) *Adv. Inorg. Biochem. 2*, 211–236.
Mildvan, A. S., Rosevear, P. R., Granot, J., O'Brian, C., Bramson, H. N., & Kaiser, E. T. (1984) *Methods Enzymol. 99*, 93–119.
Nageswara Rao, B. D., Cohn, M., & Noda, L. (1978) *J. Biol. Chem. 253*, 1149–1158.
Pai, E. F., Sachsenheimer, W., Schirmer, R. H., & Schulz, G. E. (1977) *J. Mol. Biol. 114*, 37–45.
Price, N. C., Cohn, M., & Schirmer, R. H. (1975) *J. Biol. Chem. 250*, 644–652.
Rhoads, D. G., & Lowenstein, J. M. (1968) *J. Biol. Chem. 243*, 3963–3972.
Rosevear, P. R., Bramson, H. N., O'Brian, C., Kaiser, E. T., & Mildvan, A. S. (1983) *Biochemistry 22*, 3439–3447.
Sachsenheimer, W., & Schulz, G. E. (1977) *J. Mol. Biol. 114*, 23–36.
Saran, A., Perahia, D., & Pullman, B. (1973) *Theor. Chim. Acta 30*, 31–44.
Sloan, D. L., Loeb, L. A., Mildvan, A. S., & Feldmann, R. J. (1975) *J. Biol. Chem. 250*, 8913–8920.
Smith, G. M., & Mildvan, A. S. (1982) *Biochemistry 21*, 6119–6123.
Steitz, T. A., Shoham, M., & Bennett, W. S., Jr. (1981) *Philos. Trans. R. Soc. London, B 293*, 43–52.
Sundaralingam, M. (1969) *Biopolymers 7*, 821–860.
Tomasselli, A. G., & Noda, L. H. (1979) *Eur. J. Biochem. 93*, 263–270.
Tropp, J., & Redfield, A. G. (1981) *Biochemistry 20*, 2133–2140.
Wagner, O., & Wüthrich, K. (1979) *J. Magn. Reson. 33*, 675–680.
Yathindra, N., & Sundaralingam, M. (1973) *Biopolymers 12*, 2261–2277.

Production of Antibodies against Rhodopsin after Immunization with $\beta\gamma$-Subunits of Transducin: Evidence for Interaction of $\beta\gamma$-Subunits of Guanosine 5′-Triphosphate Binding Proteins with Receptor†

Jane L. Halpern,* Patrick P. Chang, Su-Chen Tsai, Ronald Adamik, Yasunori Kanaho, Robert Sohn, Joel Moss, and Martha Vaughan

Laboratory of Cellular Metabolism, National Heart, Lung, and Blood Institute, National Institutes of Health, Bethesda, Maryland 20892

Received August 13, 1986; Revised Manuscript Received November 13, 1986

ABSTRACT: The light-detecting system of retinal rod outer segments is regulated by a guanyl nucleotide binding (G) protein, transducin, which is composed of α-, β-, and γ-subunits. Transducin couples rhodopsin to the intracellular effector enzyme, a cGMP phosphodiesterase. The $\beta\gamma$ complex ($T_{\beta\gamma}$) is required for the α-subunit (T_α) to interact effectively with the photon receptor rhodopsin. It is not clear, however, whether $T_{\beta\gamma}$ binds directly to rhodopsin or promotes T_α binding to rhodopsin only by binding to T_α. We have found that serum from rabbits immunized with $T_{\beta\gamma}$ contained a population of antibodies that were reactive against rhodopsin. These antibodies could be separated from $T_{\beta\gamma}$ antibodies by adsorbing the latter on immobilized transducin. Binding of purified rhodopsin antibodies was inhibited by $T_{\beta\gamma}$, suggesting that the rhodopsin antibodies and $T_{\beta\gamma}$ bound to the same site on rhodopsin. We propose that the rhodopsin antibodies act both as antiidiotypic antibodies against the idiotypic $T_{\beta\gamma}$ antibodies and as antibodies against rhodopsin. This hypothesis is consistent with the conclusion that $T_{\beta\gamma}$ interacts directly with the receptor. It is probable that in an analogous way, $G_{\beta\gamma}$ interacts directly with receptors of the adenylate cyclase system.

In the light-detecting system of retinal rod outer segments, the photon receptor rhodopsin is coupled with the effector enzyme cGMP phosphodiesterase through transducin, a GTP-binding regulatory (G)[1] protein (Stryer et al., 1981). Activation of rhodopsin by light stimulates binding of GTP to transducin (Fung & Stryer, 1980) which can then activate the phosphodiesterase. With hydrolysis of the bound GTP, transducin returns to the inactive state. Transducin has significant structural and functional homology with the stimulatory and inhibitory G proteins, G_s and G_i, respectively, that regulate the hormone-sensitive adenylate cyclase (Gilman, 1984; Lefkowitz et al., 1984). These G proteins are heterotrimers with α-, β-, and γ-subunits (Hildebrandt et al., 1984; Bokoch et al., 1984; Fung et al., 1981). The α-subunits bind and hydrolyze GTP (Gilman, 1984; Fung et al., 1981). Examination of cDNA clones for T_α, $G_{i\alpha}$, and $G_{s\alpha}$ has revealed striking homology (Medynski et al., 1985; Tanabe et al., 1985;

† This work was presented in part at a meeting of the Association of American Physicians in May 1985 (Chang et al., 1985).

* Address correspondence to this author.

[1] Abbreviations: G proteins, guanyl nucleotide binding regulatory proteins; G_s and G_i, stimulatory and inhibitory G proteins, respectively, of adenylate cyclase; $G_{s\alpha}$ and $G_{i\alpha}$, α-subunits, respectively, of G_s and G_i; $G_{\beta\gamma}$, β- and γ-subunits of G_s and G_i; T_α and $T_{\beta\gamma}$, α- and $\beta\gamma$-subunits of transducin; ELISA, enzyme-linked immunosorbent assay; TBS, Tris-buffered saline; TTBS, Tris-buffered saline with 0.05% Tween-20; buffer A, 0.15 M Na_2HPO_4, pH 8.5; buffer B, 2.7 mM KCl/1.5 mM KH_2PO_4/150 mM NaCl/8 mM Na_2HPO_4; buffer C, buffer B containing 0.001% Triton X-100, 2 mM EDTA, and 1% horse serum; Tris, tris(hydroxymethyl)aminomethane; EDTA, ethylenediaminetetraacetic acid; SDS, sodium dodecyl sulfate.